

Quantum magnetic properties of the SU(2N) Hubbard model in the square lattice: a quantum Monte Carlo study

Zi Cai,^{1,2} Hsiang-Hsuan Hung,^{3,1} Lei Wang,⁴ and Congjun Wu¹

¹*Department of Physics, University of California, San Diego, CA92093*

²*Department of Physics and Arnold Sommerfeld Center for Theoretical Physics, Ludwig-Maximilians-Universität München, Theresienstr. 37, 80333 Munich, Germany*

³*Department of Electrical and Computer Engineering, University of Illinois, Urbana, Illinois 61801*

⁴*Theoretische Physik, ETH Zurich, 8093 Zurich, Switzerland*

We employ the determinant projector quantum Monte-Carlo method to investigate the ground state magnetic properties in the Mott insulating states of the half-filled SU(4) and SU(6) Fermi-Hubbard model in the 2D square lattice, which is free of the sign problem. The long-range antiferromagnetic Neel order is found for the SU(4) case with a small residual Neel moment. Quantum fluctuations are even stronger in the SU(6) case. Numeric results are consistent with either a vanishing or even weaker Neel ordering than that of SU(4).

PACS numbers: 71.10.Fd, 02.70.SS, 03.75.Ss, 37.10.Jk, 71.27.+a

Quantum antiferromagnetism (AF) has been an important topic of the two-dimensional (2D) strongly correlated systems for decades. For the Hubbard model in the 2D square lattice, charge gap opens starting from an infinitesimal U . The low energy physics is described by the AF Heisenberg model. For the SU(2) case, quantum spin fluctuations are not strong enough to suppress AF long-range order^{1,2}. Augmenting the symmetry to SU(N) or Sp($2N$) enhances quantum spin fluctuations³⁻⁵, which can be handled by the systematic $1/N$ -analysis. The SU(N) spin operators can be formulated in terms of either bosonic or fermionic representations. The bosonic large- N analysis finds gapped quantum paramagnetic states exhibiting various crystalline orderings⁶, while the fermionic one gives rise to gapless flux-type spin liquid states^{4,7}. However, its stability remains an open issue. On the other hand, short-range resonating-valence-bond type gapped spin liquid states have also been extensively studied⁸⁻¹⁰.

Due to the difficulty of handling strong correlations, numerical simulations have been playing an important role on the study of exotic quantum spin states¹¹⁻¹⁹. Whether the spin-disordered quantum insulating states exist in the honeycomb lattice or not is currently under debating^{15,20}. A constrained path-integral quantum Monte-Carlo (QMC) simulation finds the evidence of a gapless spin disordered phase in the square lattice with π -flux per plaquette¹⁶. Evidence of gapped spin liquid phases has also been found by the density-matrix-renormalization-group simulations of the frustrated Heisenberg models in the Kagome lattice¹⁷ and in the square lattice with diagonal couplings¹⁸.

The Fermi-Hubbard models with $2N$ components possessing the SU($2N$) or Sp($2N$) symmetries are not only of academic interest now, but also have become the goal of experimental efforts in the ultra-cold atom physics²¹. It was first proposed to use large-spin alkali and alkaline-earth atoms to realize the Sp($2N$) and SU($2N$) Hubbard models in Ref. [22] for the special case of $2N = 4$

with the proof of a generic Sp(4) symmetry without fine-tuning. Currently, the SU(6) and SU(10) symmetric systems of ¹⁷³Yb and ⁸⁷Sr atoms have been realized, respectively²³⁻²⁵. In particular, the ¹⁷³Yb atoms have been loaded into optical lattices to realize the SU(6) Hubbard model, and the charge excitation gap has been observed²⁴. It has also been expected that Pomeranchuk cooling is efficient in the large- N case to further cool the system down to the temperature scale of the AF exchanges²⁶.

In this article, we investigate the magnetic properties of the half-filled SU($2N$) Hubbard models with $2N = 4$ and 6 by the sign-problem free determinant projector quantum Monte-Carlo (QMC) method. For the SU(4) case, the ground state remains AF ordered as in the case of SU(2) although the residual spin moments are much weaker. For the SU(6) case, we find that the residual Neel moments are either absent or extremely small beyond the resolution limit of our simulations on structure factors and the finite size scaling scheme.

The SU($2N$) Fermi Hubbard model in the 2D square lattice at half-filling is defined as

$$H = -t \sum_{\langle i,j \rangle, \alpha} \left\{ c_{i\alpha}^\dagger c_{j\alpha} + h.c. \right\} + \frac{U}{2} \sum_i (n_i - N)^2, \quad (1)$$

where t is scaled as 1 below; α represents spin indices running from 1 to $2N$; $\langle i, j \rangle$ denotes the summation over the nearest neighbors; n_i is the particle number operator on site i defined as $n_i = \sum_{\alpha=1}^{2N} c_{i\alpha}^\dagger c_{i\alpha}$. Eq. 1 is invariant under the particle-hole transformation in bipartite lattices as $c_{i\alpha} \rightarrow (-)^i c_{i\alpha}^\dagger$, and thus the average filling per site $\langle n_i \rangle = N$. Similarly to the case of SU(2), the SU($2N$) Hubbard model at half-filling in bipartite lattices is free of the sign problem for an arbitrary value of $2N$.

We use the determinant projector QMC method for fermions with the periodical boundary condition²⁷⁻²⁹. The simulated system sizes $L \times L$ range from $L = 4$ to 16. Finite-size scaling is performed to extrapolate the ground state properties in the thermodynamic limit. The initial

trial wavefunction is the ground state of the free part of Eq. 1 whose hopping integral is attached a small flux to break the degeneracy¹⁵. Such a Slater-determinant plane-wave state for the imaginary-time evolution is assumed to be non-orthogonal to the true ground state of the entire Hamiltonian. The second order Suzuki-Trotter decomposition is performed with the imaginary time-step $\Delta\tau = 0.05$. The convergence of the simulation results with respect to different values of $\Delta\tau$ has been checked. The length of the imaginary-time evolution is $\beta = 40$. For the SU(2) case, the Hubbard-Stratonovich (HS) transformation is usually performed by using the discrete Ising spin fields¹. However, the spin channel decomposition does not easily generalize to the SU(2N) case due to the increasing of spin components. Instead, we follow the approximate discrete HS decomposition in the density channel at the price of involving complex numbers³⁰. The error of this approximation is at the order $(\Delta\tau)^4$, smaller than that of the Suzuki-Trotter decomposition, thus is negligible. This method has the advantage that the SU(2N) symmetry is maintained explicitly, and also it easily generalizes to large values of $2N$.

Let us fix the convention of the SU(2N) generators. The Hilbert space on site i filled with r ($1 \leq r \leq 2N$) fermions forms the SU(2N) representation described by the single column Young pattern denoted as 1^r where r is the number of rows. For these 1^r -representations, the SU(2N) generators are defined as

$$J^{\alpha\beta}(i) = c_{\alpha}^{\dagger}(i)c_{\beta}(i) - \frac{\delta_{\alpha\beta}}{2N} \sum_{\gamma=1}^{2N} c_{\gamma}^{\dagger}(i)c_{\gamma}(i). \quad (2)$$

Another standard definition is through the generalized Gell-mann matrices $c_{\alpha}^{\dagger}(i)\lambda_{\alpha\beta}^a c_{\beta}(i)$ with $1 \leq a \leq 4N^2 - 1$ and the normalization condition of $\text{tr}[\lambda^a \lambda^b] = \frac{1}{2}\delta^{ab}$. The definition in Eq. 2 has a simple commutation relation as $[J^{\alpha\beta}, J^{\gamma\delta}] = \delta_{\beta\gamma}J^{\alpha\delta} - \delta_{\alpha\delta}J^{\gamma\beta}$. However, the price is that not all of the operators of Eq. 2 are independent, which satisfy the constraint $\sum_{\alpha} J^{\alpha\alpha} = 0$. The quadratic Casimir operator is expressed as $C_2(2N) = \frac{1}{2} \sum_{\alpha\beta} J^{\alpha\beta}(i)J^{\beta\alpha}(i)$. For the 1^r representation denoted by the Young pattern with a single column with r boxes, its value is related to the filling number r through the Fierz identity as $C_2(2N, r) = r(2N - r)(2N + 1)/(4N)$. In the large U limit in which charge fluctuations are negligible, each site represents the self-conjugate representation 1^N . The two-site equal time spin-spin correlation function is defined as

$$C_{J, SU(2N)}(i, j) = \frac{1}{C_2(2N, N)} \sum_{\alpha, \beta} \frac{1}{2} \langle J^{\alpha\beta}(i)J^{\beta\alpha}(j) \rangle, \quad (3)$$

where $C(2N, N) = N(2N + 1)/4$ is the Casimir for 1^N representation. $C_{J, SU(2N)}(i, i)$ approaches 1 in the large U -limit. The normalized spin structure factor at the AF

wavevector \vec{Q} is defined as

$$S_{SU(2N)}(\vec{Q}) = \frac{1}{C_2(2N, N)} \sum_{\alpha\beta} \frac{1}{2} \langle J^{\alpha\beta}(\vec{Q})J^{\beta\alpha}(\vec{Q}) \rangle, \quad (4)$$

where $J^{\alpha\beta}(\vec{Q}) = \frac{1}{L} \sum_i e^{i\vec{Q}\cdot\vec{r}_i} J^{\alpha\beta}(i)$. The imaginary-time-displaced spin-spin correlations at wavevector \vec{Q} are defined as

$$S_{SU(2N)}(\vec{Q}, \tau) = \sum_{\alpha\beta} \langle J^{\alpha\beta}(\vec{Q}, \tau)J^{\beta\alpha}(\vec{Q}, 0) \rangle, \quad (5)$$

which are used to extract spin gaps below.

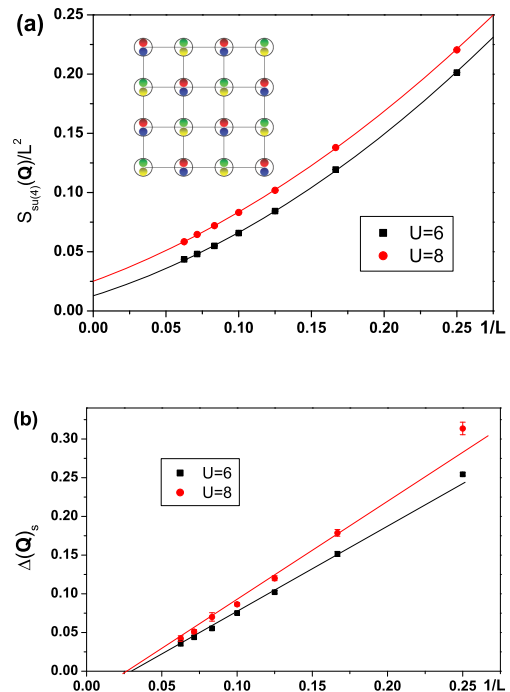


FIG. 1: The half-filled SU(4) Hubbard model in the square lattice. (a) The appearance of the AF long-range-order from the finite size scaling of the spin structure factor at $\vec{Q} = (\pi, \pi)$ for $U = 6$ and 8. Solid curves are quadratic fits of data. The inset shows a typical SU(4) AF configuration in which different colors represent different spin components. (b) The absence of the spin gap from the finite size scaling of $\Delta_s(\vec{Q})$.

The SU(4) case Below we present the study of quantum spin fluctuations starting with the SU(4) case in the square lattice, in which we find long-range AF ordering since intermediate values of U . The finite size scaling of the spin structure factor $\frac{1}{L^2} S_{SU(4)}(\vec{Q})$ at the AF wavevector $\vec{Q} = (\pi, \pi)$ is plotted in Fig. 1 (a). For example, at $U = 8$, it extrapolates to a small but finite value of $s_0 = 0.025$ as $L \rightarrow \infty$, which indicates the existence of the AF long-range Neel order. In comparison, for the SU(2) case at the same value of U , the extrapolated value of $\lim_{L \rightarrow \infty} \frac{1}{L^2} S_{SU(2)}(\vec{Q}) \approx 0.118$. This shows

the enhancement of quantum spin fluctuations as $2N$ increases.

Let us bipartite the lattice into A and B sublattices. One typical classic $SU(4)$ Neel configuration is that A -sites are filled with components 1 and 2, and B -sites filled with components 3 and 4. $SU(4)$ is a rank-3 Lie group, and thus its Cartan algebra has three commutable generators defined as $K_{1,2} = \frac{1}{2\sqrt{2}}[(n_1 - n_2) \pm (n_3 - n_4)]$, and $K_3 = \frac{1}{2\sqrt{2}}[(n_1 + n_2) - (n_3 + n_4)]$. Each site of the above $SU(4)$ configuration is a singlet of $K_{1,2}$, and with the eigenvalues of $\pm \frac{1}{\sqrt{2}}$ for K_3 . The AF long-range-ordered states possess gapless Goldstone modes, and the Goldstone manifold is the 8-dimensional Grassmann one $U(4)/[U(2) \times U(2)]$. The spin excitations carry quantum numbers of $K_{1,2,3}$ as $(\pm \frac{1}{\sqrt{2}}, 0, \pm \frac{1}{\sqrt{2}})$ and $(0, \pm \frac{1}{\sqrt{2}}, \pm \frac{1}{\sqrt{2}})$. To verify the absence of spin gap, we calculate the imaginary-time-displaced spin correlation function $S_{SU(4)}(\vec{Q}, \tau)^{31,32}$. The finite size spin-gap $\Delta_s(\vec{Q}, 1/L)$ is fitted from the slope of $\ln S_{SU(4)}(\vec{Q}, \tau)$ v.s. τ . The finite-size scaling is plotted in Fig. 1 (b) which shows the absence of spin gap in consistent with the long-range AF ordering.

The $SU(6)$ case As $2N$ increases to 6, quantum spin fluctuations become even stronger. The QMC simulation of the spin structure factors at $\vec{Q} = (\pi, \pi)$ is presented in Fig. 2 (a). The finite size scalings of the $SU(6)$ AF structure factor for all the cases of $U = 4, 8$ and 12 extrapolate to zero. However, because the $1/L$ extrapolation of the AF structure factor is proportional to the square of the AF moments, the possibility of a weak AF long-range-order cannot be excluded. For example, a Neel moment at the order of 10^{-2} corresponds to the structure factor at the order of 10^{-3} or 10^{-4} , which is beyond our current resolution limit. We further calculate the spin gap value at $\vec{Q} = (\pi, \pi)$ from the imaginary-time-displaced $SU(6)$ spin correlation function $S_{SU(6)}(\vec{Q}, \tau)$, and plot the extracted spin gap values in Fig. 2 (b). The finite-size scaling shows the vanishing of spin gap in the $SU(6)$ case for all the three values of $U = 4, 8$ and 12 . The vanishing of spin gaps are also consistent with very small but nonzero AF moments. The two-point equal-time spin-spin correlations $C_{J,SU(6)}(L/2, L/2)$ are calculated and plotted in Fig. 2 (c), which are fitted with algebraic correlations as $C_{J,SU(6)}(L/2, L/2) \approx L^{-\eta}$. However, due to the limited sample size, these algebraic correlations are well fitted at a intermediate length scale. We still cannot exclude the possibility of small long-range AF moments.

We further check other possible ordering patterns involving two neighboring sites. At half-filling, total particle number on a bond is $2N$, which is sufficient to form an $SU(2N)$ singlet to minimize the spin superexchange energy. We consider ordering patterns in the spin singlet channel with translational symmetry breaking. The bond dimer and current operators are defined as the real and imaginary parts of the hopping amplitudes between

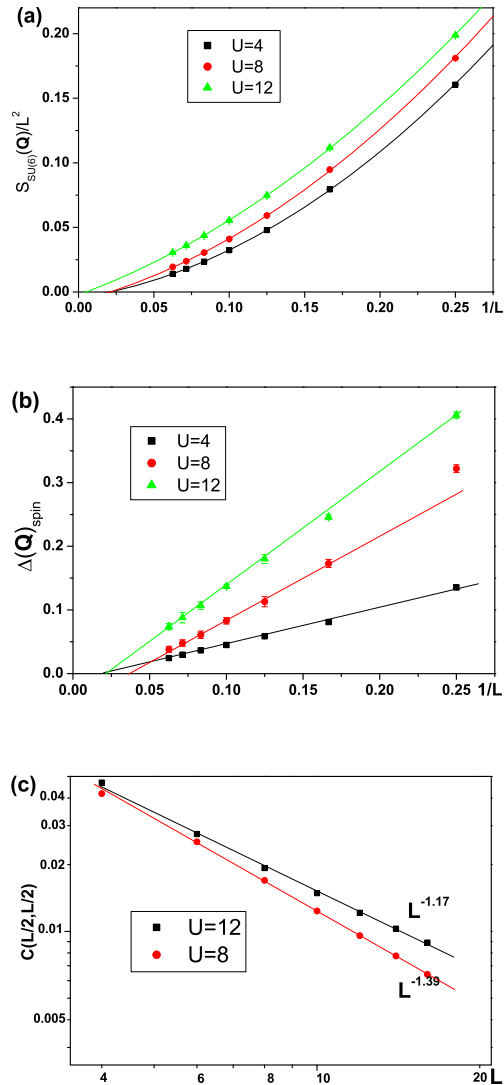


FIG. 2: Spin correlations of the half-filled $SU(6)$ Hubbard model. (a) The finite-size scalings of the spin structure factors at $\vec{Q} = (\pi, \pi)$ at $U = 4, 8$ and 12 are consistent with either zero or a very weak Neel ordering. Solid curves are quadratic fits. (b) The finite-size scalings $\Delta_s(\mathbf{Q})$ show the absence of spin gap. (c) The scalings of the farthest point correlations $C_{J,SU(6)}(L/2, L/2)$ for $U = 8$ and 12 .

nearest neighbors as

$$D_{ij} = \sum_{\alpha} c_{i,\alpha}^{\dagger} c_{j,\alpha} + h.c., \quad F_{ij} = \sum_{\alpha} i(c_{i,\alpha}^{\dagger} c_{j,\alpha} - h.c.), \quad (6)$$

and d -density-wave (DDW) operators as $DDW(i) = (-)^i \sum_j F(i, j)$ where $\vec{r}_j - \vec{r}_i = \pm \hat{e}_x$, and $\pm \hat{e}_y$. In the large U limit, the Heisenberg term $S^{\alpha\beta}(i)S^{\beta\alpha}(j)$ is generated from the second order virtual hopping process, thus D_{ij} can be used as the dimer order parameter. The structure factor of D_{ij} at $\vec{Q}' = (\pi, 0)$ and that of DDW

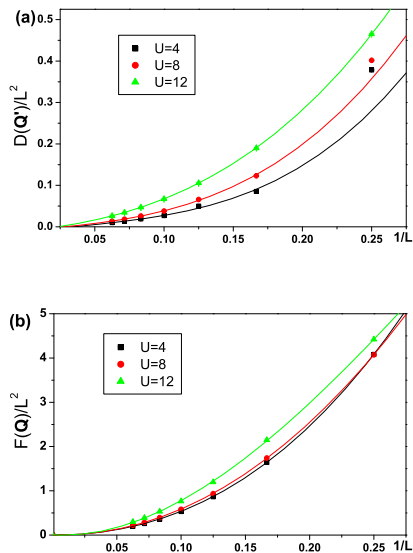


FIG. 3: Spin singlet channel operators of the half-filled SU(6) Hubbard model. (a) The finite-size scaling of the columnar dimer structure factors at $\vec{Q}' = (\pi, 0)$. (b) The finite-size scaling of the DDW structure factors at $\vec{Q} = (\pi, \pi)$.

at $\vec{Q} = (\pi, \pi)$, after divided by L^2 , and are plotted in Fig. 2 b) and c), respectively. They are fitted by a power-law $(1/L)^2$, thus their correlations are short-ranged.

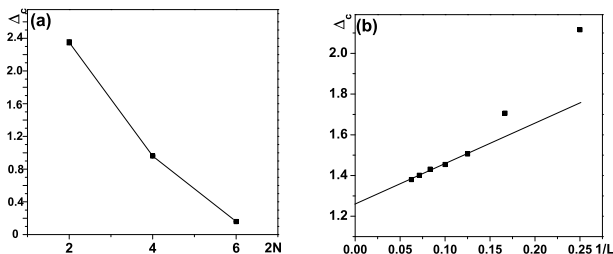


FIG. 4: Single-particle gaps of half-filled SU(2N) Hubbard models. A) Charge gaps with $U = 8$ at $2N = 2, 4$ and 6 . B) The $1/L$ scaling of the charge gap for the half-filled SU(6) model at $U = 12$.

Single-particle gaps The single-particle gaps for the SU(4) and SU(6) Hubbard models are also calculated at half-filling through the onsite imaginary time-displaced Green's function $G(0, \tau) = \frac{1}{L^2} \sum_i \langle \Psi_G | c(i, \tau) c^\dagger(i, 0) | \Psi_G \rangle$, where $|\Psi_G\rangle$ is the ground state. At long time displacement, $G(0, \tau) \rightarrow e^{-\Delta_c \tau}$ where Δ_c is the single-particle excitation gap, thus Δ_c can be fitted from the slope of $\ln G(0, \tau)$ v.s. τ . Let us consider the large U -limit for an intuitive picture: in the Mott-insulating background, the energy of adding a particle is lowered from U by further virtual particle-hole excitations. In other words, the Mott-insulator is polarizable. As increasing $2N$, the configuration numbers of the virtual particle-hole excitations increase, which enhances charge fluctuations and thus reduces the single-particle gap. In Fig. 4 (a), Δ_c 's are plotted at a fixed $U = 8$ for $2N = 2, 4$ and 6 , all of which are finite. For the SU(6) case, $\Delta_c = 0.15$ is rather small at $U = 8$. Nevertheless, Δ_c increases to 1.26 at $U = 12$ at which the system is safely inside the Mott-insulating regime. The charge localization length can be estimated as $\xi_c \approx v_f / \Delta_c \approx 3 \sim 4$ which is much smaller than the maximal sample size $L = 16$.

In conclusion, we have studied the ground state quantum antiferromagnetism in a half-filled SU(2N) Hubbard model in square lattice. For the case of SU(4), a long-range AF order still survives with a much smaller value of Neel moment compared to that of SU(2). For the SU(6) case, we have found the absence of spin gap. The current numeric results are consistent with either a vanishing or very weak AF ordering beyond the resolution limit in this simulation. We have also found that the single particle gap is strongly suppressed as increasing N .

C. W. thanks J. Hirsch and S. Kivelson for very helpful discussions. Z.C thanks F.F. Assaad for helpful discussion. Z. C., Y. L. and C. W. are supported by the NSF DMR-1105945 and the AFOSR FA9550-11-1-0067(YIP program).

¹ J. E. Hirsch, Phys. Rev. B **31**, 4403 (1985).
² J. E. Hirsch, and S. Tang, Phys. Rev. Lett. **62**, 591 (1989).
³ D. P. Arovas and A. Auerbach, Phys. Rev. B **38**, 316 (1988).
⁴ I. Affleck and J. B. Marston, Phys. Rev. B **37**, 3774 (1988).
⁵ S. Sachdev and N. Read, Int. J. Mod. Phys. B **5**, 219 (1991).
⁶ N. Read and S. Sachdev, Nucl. Phys. B **316**, 609 (1989); N. Read and S. Sachdev, Phys. Rev. Lett. **66**, 1773 (1991).
⁷ M. Hermele, T. Senthil, M. P. A. Fisher, P. A. Lee, N.

Nagaosa, and X. G. Wen, Phys. Rev. B **70**, 214437 (2004).
⁸ P. W. Anderson, Mat. Res. Bull. **8**, 153 (1973).
⁹ D.S. Rokhsar and S.A. Kivelson, Phys. Rev. Lett. **61**, 2376 (1988); E. Fradkin, S. A. Kivelson, Mod. Phys. Lett. B **4**, 225 (1990).
¹⁰ R. Moessner, S. L. Sondhi, Phys. Rev. Lett **86**, 1881 (2001)
¹¹ K. Harada, N. Kawashima, M. Troyer, Phys. Rev. Lett. **90**, 117203 (2003)
¹² R. K. Kaul, R. G. Melko, A. W. Sandvik, arXiv:1204.5405.
¹³ F. F. Assaad, Phys. Rev. B **71**, 075103 (2005).

- ¹⁴ A. Paramekanti, J. B. Marston, *J. Phys. Cond. Matt.* **19**, 125215 (2007).
- ¹⁵ Z. Y. Meng, T. C. Lang, S. Wessel, F. F. Assaad, A. Muramatsu, *Nature* **464**, 847 (2010).
- ¹⁶ C. C. Chang, R. T. Scalettar, *Phys. Rev. Lett.* **109**, 026404 (2012).
- ¹⁷ S. Yan, D. A. Huse, S. R. White, *Science* **332**, 1173-1176 (2011).
- ¹⁸ H. C. Jiang, H. Yao, L. Balents, *Phys. Rev. B* **86**, 024424 (2012).
- ¹⁹ N. Blümer; E.V. Gorelik, *Phys. Rev. B* **87**, 085115 (2013).
- ²⁰ S. Sorella, Y. Otsuka, and S. Yunoki, *Scientific Reports* **2**, 992 (2012).
- ²¹ C. Wu, *Physics* **3**, 92 (2010) and reference therein.
- ²² C. Wu, J. P. Hu, and S. C. Zhang, *Phys. Rev. Lett.* **91**, 186402(2003), C. Wu, *Mod. Phys. Lett. B* **20**, 1707 (2006).
- ²³ A. V. Gorshkov *et al.*, *Nature Phys.* **6**, 289 (2010).
- ²⁴ S. Taie *et al.*, *Phys. Rev. Lett.* **105**, 190401 (2010), S. Taie *et al.*, *Nature Physics*, **8**, 825 (2012).
- ²⁵ B. J. DeSalvo *et al.*, *Phys. Rev. Lett.* **105**, 030402 (2010).
- ²⁶ Zi Cai, *et al.*, arXiv:1202.6323; K. R. A. Hazzard *et al.*, *Phys. Rev. A* **85**, 041604(R) (2012); L. Bonnes *et al.*, *Phys. Rev. Lett.* **109**, 206305 (2012).
- ²⁷ G. Sugiyama and S. Koonin, *Ann. Phys.* **168**, 1 (1986).
- ²⁸ S.R. White *et al.*, *Phys. Rev. B* **40**, 506 (1989).
- ²⁹ F. Assaad and H. Evertz, Computational Many-Particle Physics (Lect. Notes Phys. 739, Springer, ADDRESS, 2008), p. 277.
- ³⁰ F. F. Assaad, ArXiv: cond-mat/9806307 (1998).
- ³¹ F. F. Assaad and M. Imada, *J. Phys. Soc. Jpn* **65**, 189 (1996).
- ³² M. Feldbacher and F. F. Assaad, *Phys. Rev. B* **63**, 073105 (2001).

